ELSEVIER

Journal of Photochemistry and Photobiology A: Chemistry 154 (2002) 81–92

Journal of Photochemistry and Photobiology A:Chemistry

www.elsevier.com/locate/jphotochem

Excited state intramolecular proton transfer in 2-(2′-hydroxyphenyl)-1H-imidazo[4,5-c]pyridine: effects of solvents

M.M. Balamurali, S.K. Dogra*

Department of Chemistry, Indian Institute of Technology Kanpur, Kanpur 208016, India

Received 3 April 2002; received in revised form 21 June 2002; accepted 25 June 2002

Abstract

Excited state intramolecular proton transfer (IPT) reaction in 2-(2′-hyrdoxyphenyl)-1H-imidazo[4,5-c]pyridine in different solvents and mixtures of binary solvents has been studied by means of UV-vis absorption, fluorescence, fluorescence excitation, time correlated single-photon counting fluorescence spectroscopy and using AM1 semi-empirical quantum mechanical calculations. Dual emission from this molecule in organic solvents under the excitation of 310 nm was observed and was ascribed to different species, rotamer a-1 and tautomer T_a, formed by the IPT in the excited S_1 state in rotamer a-2. The emission is discussed in terms of a four-state diagram in which the tautomeric form, in the ground state, is only obtained by emission from the excited tautomer and this species quickly converted into more stable species rotamer a-2. The fluorescence quantum yield of the tautomer emission decreases with the increase of polarity and hydrogen bonding nature of the solvents, whereas that of normal band increases under the similar conditions but it starts decreasing after certain composition of the solvent mixtures. Polarity of the solvents plays the major role in decreasing the fluorescence quantum yield of the tautomeric band.

Keywords: Excited state intramolecular proton transfer; Fluorescence; Phototautomer; Binary solvents

1. Introduction

Electron transfer and proton transfer reactions are the most fundamental problems in photochemistry. The latter has been studied extensively in the ground state (S_0). In recent years, there has been tremendous interest in studying the photo-physics of the photo-induced proton transfer processes in general [1] and excited state intramolecular proton transfer (ESIPT) in particular [2–14]. The latter process involves the presence of intramolecular hydrogen bond between the acidic and basic centers in S_0 state. The charge density distribution changes upon excitation of these molecules in their first excited singlet state (S_1). This introduces large changes in their acidic and basic properties and thus leads to proton transfer along the hydrogen bond in a tautomerization process. ESIPT is normally extensively fast and is nearly without any activation energy. Recently number of molecules showing ESIPT behavior have been investigated thoroughly and these molecules have been used in the action of dye lasers [15–17], polymer photo-stabilizers [18], high energy radiation detectors [19,20], molecular energy storage [21] and as fluorescent probes [22–28].

For the last two decades, we have been studying the ESIPT in 2-(2′-hyroxyphenyl)- and 2-(2′-aminophenyl)benzazoles [29–40] in the homogeneous systems and 2-(2′-hyroxyphenyl)benzimidazole (2-HPBI) [26–28] in the heterogeneous media. The fluorescence quantum yield of the tautomer band in 2-HPBI is quite large (0.55) [29] in non-polar solvents and decreases with the increase in the protic nature of the solvents. Recently we have studied the photo-physics of the ESIPT reaction in 2-(2′-hydroxyphenyl)-3H-imdazo[4,5-b]pyridine (2-HPIP-b) [41]. This molecule is different from 2-HPBI in the sense that it contains one more nitrogen atom in the benzo ring at the 7th position (Scheme 1). Our results have shown that the fluorescence quantum yields of both the bands are much less than that observed for 2-HPBI. This has been attributed to the presence of the lone pair of electrons on nitrogen atom in the benzo ring and could be due to the enhancement of the intersystem-crossing rate. A similar behavior has also been observed in 2-(2′-aminophenyl)- [42] and 2-(2′-*N*,*N*-dimethylaminophenyl)pyrido[3,4-d]imidazoles [43]. The present study describes the photo-physics of 2-(2′-hyroxypheyl)-1H-imidazo[4,5-c]pyridine (2-HPIP-c),

* Corresponding author. Tel.: +91-512-597163; fax: +91-512-590007.
E-mail address: skdogra@iitk.ac.in (S.K. Dogra).

1010-6030/02/$ – see front matter
PII: S1010-6030(02)00308-8

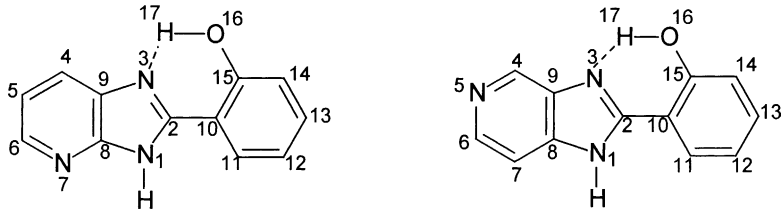

Scheme 1.

which is an isomer of 2-HPIP-b (Scheme 1). It has been observed that the acidic and basic characteristics of these kinds of isomers, where the acidic and the basic centers are similar but are placed at different positions in the aromatic ring, are very different from each other. For example, the pK_a value for the protonation reaction in benzimidazole (BI) is 5.53 [44–46], whereas that in indazole it is 1.24 [47]. These changes in the acidic and basic properties of the aromatic systems are due to different changes observed in the charge distribution on the acidic and basic centers upon excitation to S_1 and thus may also change the photo-physics of the molecules. In the present study, we report the results for 2-HPIP-c in various solvents obtained by UV-vis absorption spectroscopy, by steady-state and time-resolved fluorescence spectroscopy and by semi-empirical (AM1) calculations of ground and excited states of 2-HPIP-c isomers, rotamers and tautomers. The latter part has also included the partial exploration of the potential energy surface for the interconversion of this process.

2. Materials and methods

2-HPIP-c was synthesized by refluxing equivalent amounts of 3,4-diaminopyrdine and 2-hydroxybenzoic acid in polyphosphoric acid at 160 °C, as described in the literature [48]. 2-HPIP-c was purified by repeated crystallization from methanol. The purity of the compound was checked by sharp melting point, chemical analysis, single point on TLC, the NMR data and resemblance of the fluorescence excitation spectra recorded at different emission wavelengths in cyclohexane. Cyclohexane, ethyl acetate, 2-propanol, dioxane, acetonitrile, methanol and ether were either of spectroscopic grade or HPLC grade from E. Merck and were used as such. Commercial ethanol was purified as described in literature [49]. Triply distilled water was used for the preparation of aqueous solutions.

The procedure used to prepare the solutions, adjustment of pH was the same as described in our recent papers [36,50]. The absorption spectra were recorded on a Shimadzu UV-vis spectrophotometer equipped with a 135U chart recorder. Steady-state fluorescence and fluorescence excitation spectra were recorded on a Fluorlog-3 (ISA Jobin Yoon Spex Instruments S.A. Inc.) spectrofluorimeter and all the spectra reported were corrected one. The band pass used for recording the fluorescence and fluorescence excitation spectra were 2 nm. Lifetimes in different solutions were measured on a nanosecond single-photon counting spectrofluorimeter (PS 70/80) supplied by Applied Photo-physics, England. The electronic processing equipment and multi-channel analyzer were from Ortec and Norland, respectively. Nitrogen gas was used in the flash lamp. The flash lamp profile, defined by the full width at half the maximum (FWHM) height is 2 ns at the lamp frequency of 30 kHz. The fluorescence decay was analyzed by the reconvolution technique (software provided by IBH Consultants, UK). The computer system was an IBM-based AT386. The lifetimes so reported possess the χ^2 in the range of 1 ± 0.2 and good autocorrelation functions. The error involved in the measurements of emission lifetime, taking into account the experimental facts is 10% and 0.2 ns is the shortest lifetime which can be measured under the best conditions of the experiments. The fluorescence quantum yields (ϕ_{fl}) have been calculated from the solutions having absorbance less than 0.1, using quinine sulfate in 1 N H_2SO_4 as reference ($\phi_{fl} = 0.55$) [51]. The fluorescence excitation spectra of 2-HPIP-c in non-polar solvents, recorded at 350 and 500 nm emission have shown that the contribution to the total absorbance at 330 nm due to the rotamer a-1 is less than 5%, whereas in methanol as solvent, it is ~21%. Thus the ϕ_{fl}^{T} of the tautomer emission in non-polar solvents at excitation wavelength (λ_{exc}) 330 nm will be close to the true value. Whereas the ϕ_{fl}^{N} values obtained in polar/protic solvents at $\lambda_{exc} = 330$ nm or in all the solvents at $\lambda_{exc} = 310$ nm have been calculated using the absorbance at these wavelengths. The concentration of 2-HPIP-c was kept at 0.6×10^{-5} M.

3. Semi-empirical calculations

Two isomers of 2-HPIP-c (labeled as ‘a’ and ‘b’) and two rotamers and one tautomer of each were considered. These are depicted in the Scheme 2. The PCMODEL program [52] was used to find the initial geometry of each species. This program helped us to draw the structure of each species, optimized roughly the geometry using MM2 force field and generates the corresponding coordinates. Using these

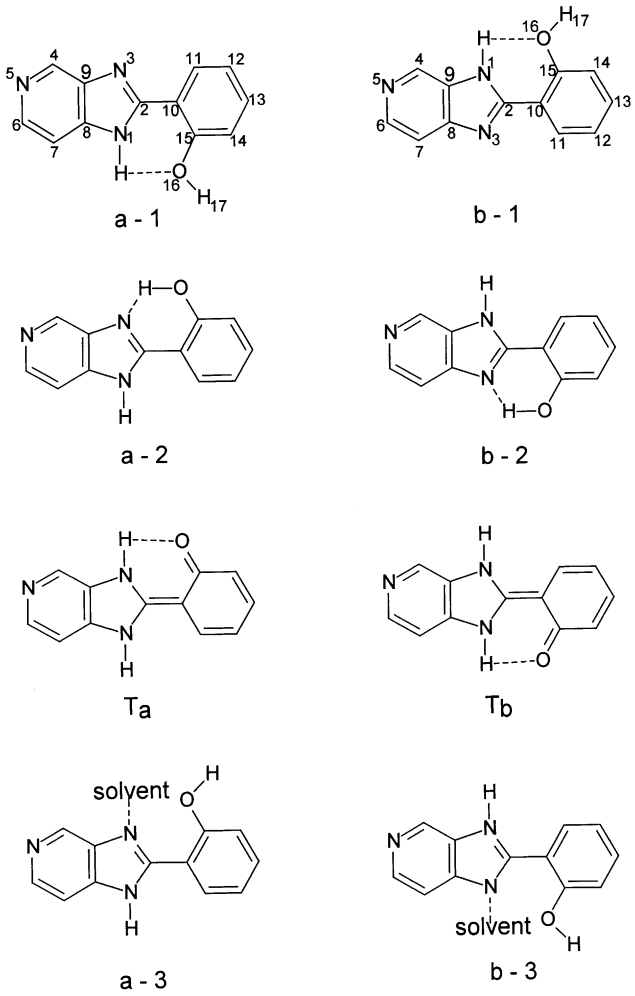

Scheme 2.

coordinates, the ground state geometry of all the species were then optimized using AM1 method (QCMP137, MOPAC 6/PC) [53]. As suggested and found by others [36,50,54–57], this method provides acceptable approximations to give results, which are quite close to the experimental findings. The ground state heat of formations (ΔH_f°), the total energy (E), dipole moment (μ), dihedral angle (N_1–C_2–C_{10}–C_{11}, φ) and the charge density at each basic center have been compiled in Table 1. For the excited states, we have followed CNDO/S-CI procedure [58], where by we have considered 64 configurations for the single electronic transitions. These configurations have been obtained by taking into account the first eight highest occupied molecular orbital (HOMO) and the first eight lowest unoccupied molecular orbital (LUMO). These calculations provided the transition energies (ΔE_{ij}). ΔE_{ij} corresponds to the excitation of an electron from the orbital ϕ_i (occupied in the ground state) to the orbital ϕ_j (unoccupied in the ground state). The total energy of the excited state (E_j) was obtained by the expression $E_j = E_i + \Delta E_{ij}$. The CI wave functions were used to generate orbitals and the one-electron density matrices. These one-electron density matrices were then used to calculate the dipole moments of the excited states of each species. The first two transitions along with their dipole moments are compiled in Table 1. The charge densities in the S_1 state at all the basic centers have also been obtained by CNDO/S-CI method [59] and are given in Table 1.

Dipolar solvation energies for different states have been calculated using the following expression based on Onsager's theory [60,61]:

$$\Delta E_{\text{solv}} = -(\mu^2)\frac{f(D)}{a^3}$$

where $f(D) = (D-1)/(2D+1)$, D the dielectric constant of the solvent, μ the dipole moment in the respective state and a the Onsager's cavity radius. For non-spherical molecules, like 2-HPIP-c, the value of a has been obtained by taking 40% of the maximum length of the molecule [62]. The maximum length of the molecule was obtained from the optimized geometry of 2-HPIP-c and the value obtained is 0.436 nm. It may be mentioned here that we have not taken into account the specific solvent interactions like hydrogen bonding, etc. for calculating the total energies. The total energies including the dipolar solvation energies for each species in methanol are also compiled in Table 1.

Relative stability of different rotamers have been obtained by presetting the dihedral angle (N_1–C_2–C_{10}–C_{11}, φ) between the hydroxyphenyl plane and the aromatic heterocyclic plane to different values and then fully optimizing all the parameters. Energies so obtained for each rotamer is plotted in Fig. 1 as a function of φ, which describes the potential energy curve for the interconversion of a-1 to a-2 in the S_0. Similarly the potential energy curve for the interconversion of a-1 to a-2 in the S_1 state was also constructed as a function of φ by adding the transition energies (ΔE_{ij}, calculated using the standard CNDO/S-CI method) to the respective ground state energy (E_i). The values of the dihedral angles obtained for the minimum energy of the rotamers a-1 and a-2 from Fig. 1 agree with those obtained by the optimization process. Similar interconversion potential energy curves for b-1 to b-2 were also obtained but are not shown.

The possibility of the interconversion of the enolic rotamer a-2 to the keto tautomer T_a by intramolecular proton transfer (IPT) along the hydrogen bond was studied by partial exploration of the potential energy surface in S_0 and S_1 states with O–H distance as the reaction coordinate. For the generation of the potential energy surface for the IPT process (interconversion of the enol form to the keto form), we have optimized the geometries with various preset values of the O–H bond distance in the S_0 state. For the generation of the similar potential energy surface for the S_1 state, we have followed the similar procedure as described above for the generation of the potential energy curve for the interconversion of a-1 to a-2 in the S_1. Fig. 2 represents the plot of the total energy versus O–H bond distance in S_0 and S_1 states under isolated conditions.

Table 1
Calculated properties of 2-HPIP-c isomers, rotamers and tautomers in the ground and excited states

Characteristics	a-1	a-2	T_a	b-1	b-2	T_b
ΔH_f° (kJ mol^{-1})	243.8	247.4	289.1	246.4	250.1	288.5
E (S_0, eV)	−2599.6942	−2599.6572	−2599.2246	−2599.6665	−2599.6295	−2599.2305
E_{solv} (S_0, eV)	−2599.8260	−2599.7402	−2599.3085	−2599.7704	−2599.6727	−2599.3185
μ_g (D)	5.99	4.72	4.78	5.30	3.43	3.07
Dihedral angle, φ (N_1–C_2–C_{10}–C_{11}) (°)	32	−138	1	28	40	0.2
R(C_2–C_{10}) (Å)	1.46	1.46	1.40	1.47	1.46	1.41
Transition energy (nm)						
S_0–S_1	315	308	393	313	308	381
S_0–S2	289	284	281	283	278	259
μ_e (D)						
S_1	7.76	6.68	4.98	5.42	4.48	3.99
S2	7.79	6.52	2.19	0.69	1.09	5.29
Charge densities						
S_0						
N_1	5.2120	5.2287	5.2595	5.2029	5.2191	5.2513
N_3	5.1249	5.1381	5.2220	5.1453	5.1638	5.2320
N_6	5.1578	5.1543	5.1285	5.1315	5.1270	5.1301
S_1						
N_1	5.2273	5.2288	5.2197	5.2012	5.2020	5.2309
N_3	5.3018	5.3071	5.2182	5.3311	5.3370	5.2054
N_6	5.2591	5.2592	5.2790	5.2219	5.2292	5.2854

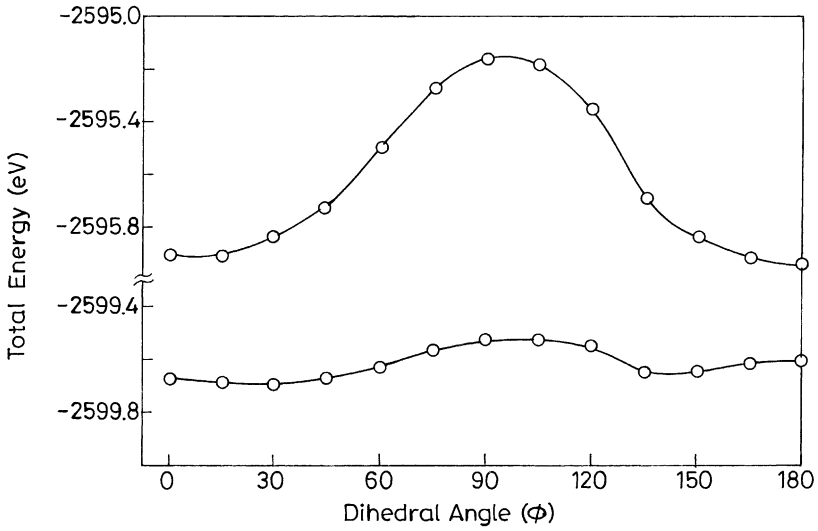

Fig. 1. Plot of total energy (E) as a function of dihedral angle (φ) in S_0 and S_1 states of the a-isomer of 2-HPIP-c under isolated conditions.

4. Results

4.1. Absorption spectrum

The absorption spectrum of 2-HPIP-c was recorded in different solvents and the relevant data are compiled in Table 2. The absorption spectra in some selected solvents are shown in Fig. 3. 2-HPIP-c was partially soluble in cyclohexane and water at pH ∼6.6 and thus molecular extinction coefficient (ε_{max}) at the band maxima of 2-HPIP-c could not be determined in these solvents. Except in water, the long wave-

Table 2
Absorption band maxima (λ_{max}^{ab}, nm) and $\log \varepsilon_{max}$ (in the parenthesis) of 2-HPIP-c in different solvents ([2-HPIP-c] = 6.0×10^{-6} M)

Solvents	λ_{max}^{ab} ($\log \varepsilon_{max}$)
Cyclohexane (satd.)	278 (sh), 285, 320, 331 (sh)
Dioxane	276 (sh), 286 (4.15), 316 (4.16), 328 (sh)
Ethyl acetate	276 (sh), 286 (4.15), 315 (4.13), 326 (sh)
Acetonitrile	279 (sh), 286 (4.19), 315 (4.16), 326 (sh)
n-Propanol	279 (sh), 285 (4.22), 316 (4.13), 325 (sh)
Ethanol	276 (sh), 286 (4.21), 316 (4.13), 325 (sh)
Methanol	279 (sh), 286 (4.21), 316 (4.13), 325 (sh)
Water (pH 6.6) (satd.)	285, 314, 320 (sh)

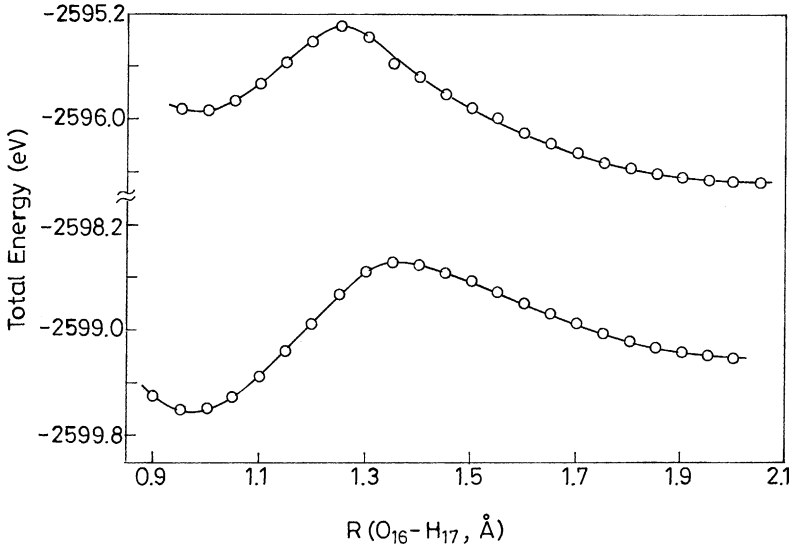

Fig. 2. Potential energy surface for intramolecular proton transfer process of 2-HPIP-c in S_0 and S_1 states under isolated conditions.

length (LW) absorption band in all the solvents consists of two peaks (one at ~328 nm and the other at ~315 nm). The short wavelength (SW) band (315 nm) is nearly insensitive to the nature of solvents, whereas the LW band (328 nm) is slightly blue shifted on increasing the polarity and hydrogen bonding capacity of the solvents. Due to very small difference in the pK_a values for the monocation–neutral (MC–N, 5.7) and the neutral–monoanion (N–MA, 9.2) [63], it is not easy to find the pH where 2-HPIP-c will be present as the neutral species. For convenience sake, we have taken pH of the solution as 6.6 in which 2-HPIP-c can be taken as close to the neutral specie. The absorption spectrum of 2-HPIP-c is broad having SW absorption band at 314 nm and shoulder at ~320 nm in water. Similar to the absorption spectrum of BI and alkyl substituted BIs [44–46], the second band system at ~278 and 285 nm are also invariant to the nature of the solvents, suggesting that the source of the LW absorption band system is due to the intramolecular hydrogen bonding (IBH) either between the >NH proton and the lone pair of the hydroxyl oxygen atom (rotamer I) or between

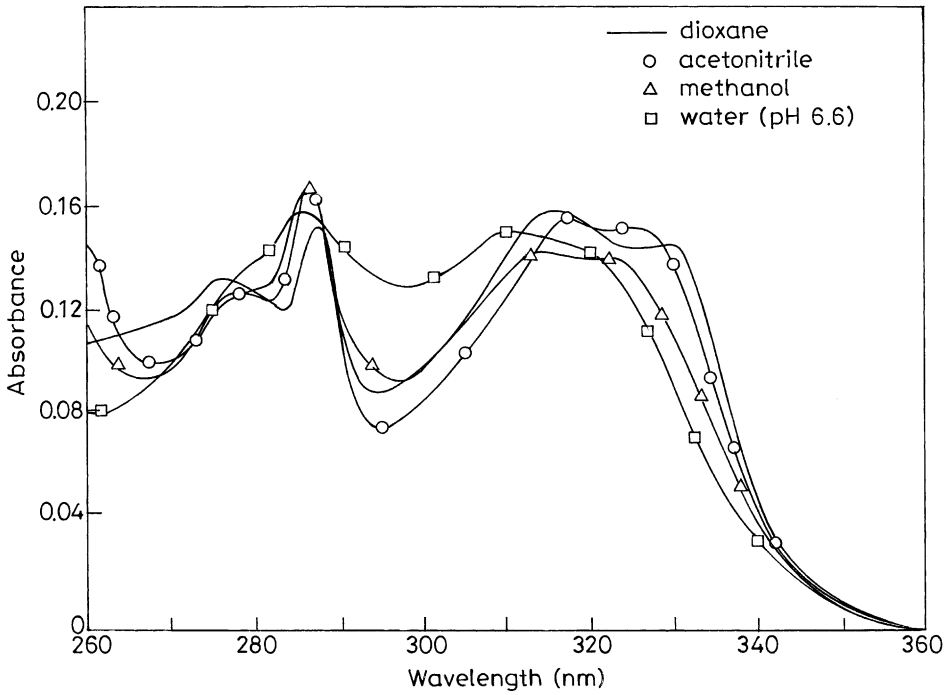

Fig. 3. Absorption spectrum of 2-HPIP-c in some selected solvents: (—) dioxane; (○) acetonitrile; (△) methanol; (□) water (pH 6.6).

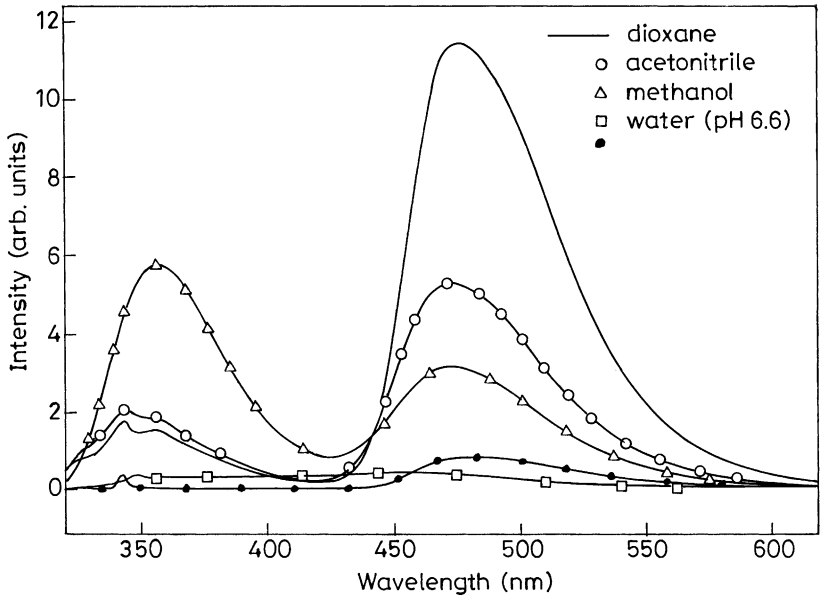

Fig. 4. Fluorescence spectrum of 2-HPIP-c in some selected solvents: (●) cyclohexane; (—) dioxane; (○) acetonitrile; (△) methanol; (□) water (pH 6.6).

the hydroxyl proton and the lone pair of the ≥N atom of the heterocyclic ring (rotamer II).

Unlike 2-HPIP-b [41], but similar to 2-HPBI [29] and 2-(3′-hydroxy-2′-pyridyl)benzimidazole (2-HpyBI) [14], a small shoulder towards the red side of the LW absorption band is observed in 2-HPIP-c in water. Detailed studies [63] (effect of λ_{exc} and pH) have shown that this shoulder is due to the presence of small amount of MA, rather than the tautomer.

4.2. Fluorescence spectra

Fluorescence spectra of 2-HPIP-c have also been studied in different solvents at two different λ_{exc} (310 and 330 nm). The fluorescence spectra in some selected solvents are shown in Fig. 4 and the relevant data are compiled in Table 3. The above results show that dual emission (342 and 477 nm, except in water) is observed in all the solvents except cyclohexane when 2-HPIP-c is excited at 310 nm and a single LW fluorescence band is observed when 2-HPIP-c is excited at 330 nm in non-polar and polar/aprotic solvents. In polar/protic solvents, dual fluorescence is observed even at $\lambda_{exc} = 330$ nm. The SW fluorescence is called the normal band and LW fluorescence band is called the tautomer band. The tautomer band is large Stoke's shifted ($\sim$9050 cm^{-1}) and structure less, whereas the normal fluorescence band is structured in non-polar solvents and the structure gets diffused in polar/protic solvents. The structure in the normal fluorescence band can be described by the vibrational frequency of 1250 ± 50 cm^{-1}. Similar emission characteristics were also observed in 2-phenyl substituted BIs [29,46] and benzoxazoles [30]. The normal band, unlike the tautomer band, is small Stokes shifted ($\sim$1200 cm^{-1} in cyclohexane, calculated from the LW fluorescence excitation band and the SW fluorescence band of the fluorescence spectrum). Relatively small Stoke's shift observed for the SW fluorescence band in non-polar solvents suggests that the molecular geometry of the rotamer 1, giving rise to the normal

Table 3
Fluorescence band maxima (λ^{fl}_{max}, nm), fluorescence quantum yields (ϕ_{fl}), of the SW and LW emission bands of 2-HPIP-c in different solvents ([2-HPIP-c] = 6×10^{-6} M)

Solvents	λ^{fl}_{max} (ϕ_{fl})	
	$\lambda_{exc} = 310$ nm	$\lambda_{exc} = 330$ nm
Cyclohexane (satd.)	477 (0.1097)	477 (0.0984)
Dioxane	327, 337, 342, 355 (0.0221), 476 (0.2022)	474 (0.2277)
Ethyl acetate	327, 337, 342, 354 (0.0261), 475 (0.2197)	474 (0.2134)
Acetonitrile	330, 344, 354 (0.0269), 474 (0.1002)	474 (0.0939)
n-Propanol	354 (0.0910) 474 (0.1651)	355 (0.0327), 474 (0.1418)
Ethanol	355 (0.0623), 472 (0.1355)	356 (0.0215), 473 (0.1332)
Methanol	356 (0.0773), 473 (0.0574)	356 (0.0319), 474 (0.0649)
Water (pH 6.6) (satd.)		458 (0.0065)

fluorescence band, do not change much on excitation to S_1 state.

The fluorescence band maxima of both the emissions are invariant to λ_{exc} in all the solvents. The invariance with respect to λ_{exc} indicates that the environment around the fluorophore is homogeneous on the time scale of the measurement over this wavelength range. Since our instrument does not have sufficient time resolution to comment on the origin of the emission in the excited states, it is thus expected that all the fluorophores should emit from the relaxed S_1 state after rapid vibrational relaxation and internal conversion. The fluorescence quantum yield of the SW fluorescence band (ϕ_{fl}^{N}) increases and that of LW fluorescence band (ϕ_{fl}^{T}) decreases with the increase in the polarity and protic nature of the solvents. The relative increase in the (ϕ_{fl}^{N}) in the protic solvents is larger than that noticed in the polar solvents. The SW fluorescence band maxima are red shifted, whereas that of LW band remains unchanged with the increase in the polarity and protic nature of the solvents, with exception of water. In water and at pH 6.6, at both the λ_{exc}, only one fluorescence band is observed (~458 nm), which is red shifted in comparison to the SW fluorescence band and blue shifted in comparison to the LW fluorescence band. Further, the fluorescence band maximum in water is red shifted with respect those of the monocation (396 nm, pH 2) and monoanion (451 nm, pH 10.9) [63]. This behavior is different from that observed in 2-HPIP-b [46], but similar to that noticed in 2-HPBI [29] and 2-(6′-hydroxy-2′pyridyl)-benzimidazole [64]. This fluorescence band in water at pH 6.6 is assigned to zwitterion, because in general the order of the band maxima observed in these species are: λ_{max}^{fl} (tautomer) > λ_{max}^{fl} (zwitterion) > λ_{max}^{fl} (monoanion) > λ_{max}^{fl} (monocation) > λ_{max}^{fl} (normal) [29,64,65].

To find the origin of the fluorescence bands, the fluorescence excitation spectra of 2-HPIP-c were recorded in many solvents ranging from non-polar (ultra dry cyclohexane) to polar/aprotic and polar/protic solvents at different emission wavelengths varying from 340 to 520 nm. As an illustration, Fig. 5 represents the fluorescence excitation spectra of 2-HPIP-c in dioxane and methanol at 340 and 520 nm. It is obvious from Fig. 5 that the fluorescence excitation spectra of normal emission are different from those of the tautomer emission in both the solvents. This suggests that the respective emission is observed by exciting different rotamers in the ground state. Further (i) the fluorescence excitation band maximum recorded at the SW emission band gets red shifted, whereas that of LW emission band gets blue shifted with the increase in the polarity of the solvents; and (ii) in the fluorescence excitation spectrum in polar protic solvents, a red shifted shoulder (357 nm) to 326 nm appears when λ_{em} ~ 450 nm. This is similar to the fluorescence excitation spectrum recorded in the basic medium and to the absorption spectrum of the monoanion. This suggests the presence of small amount of monoanion in these media [63]. The intensity of the 357 nm fluorescence excitation band decreases if λ_{em} is increased.

4.3. Solvatochromic effect

It is mentioned earlier that the SW fluorescence band is red shifted and LW fluorescence band is invariant to the solvent polarity. This suggests that there is hardly any change in the dipole moment of the rotamer, responsible for the formation of tautomer, when excited to S_1, whereas the dipole moment of the rotamer responsible for the normal fluorescence band increases on excitation to S_1 state. Lippert plot [66,67] was

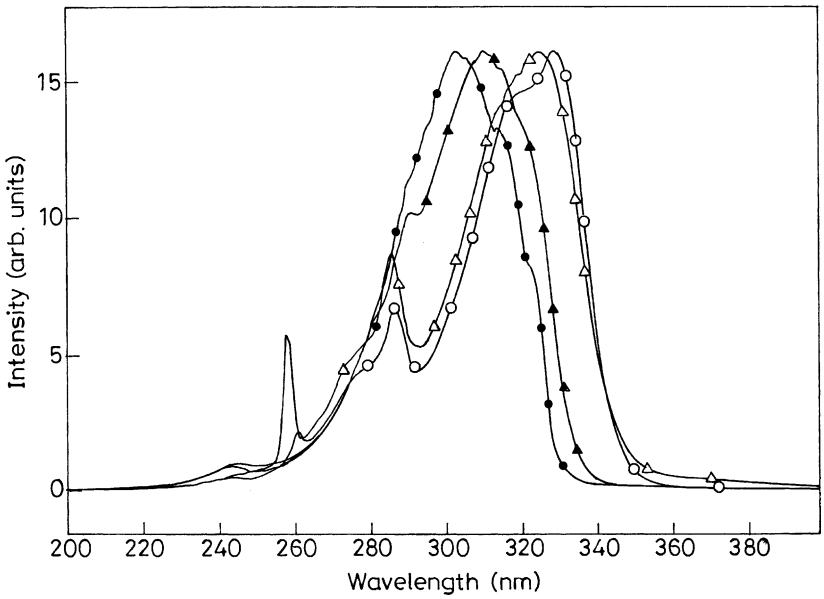

Fig. 5. Fluorescence excitation spectrum of 2-HPIP-c recorded at λ_{em} 340 and 520 nm in dioxane and methanol. In dioxane (●), λ_{em} 340 nm and (○), λ_{em} 520 nm; in methanol (▲), λ_{em} 350 nm and (△), λ_{em} 520 nm.

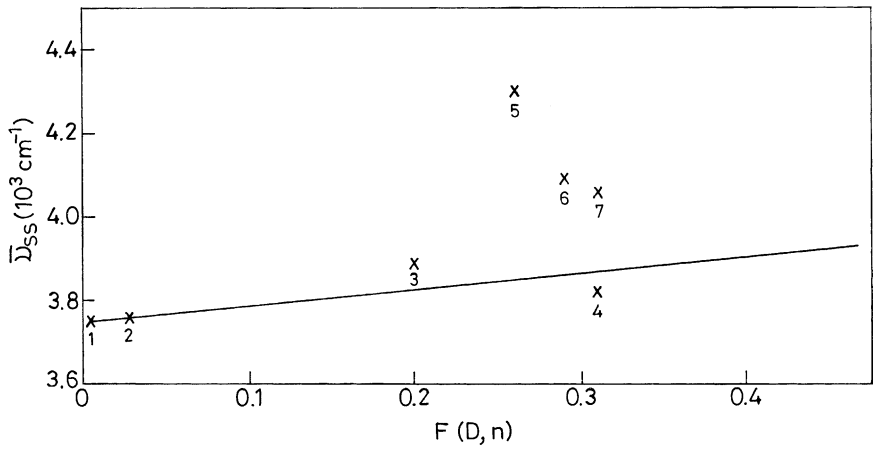

Fig. 6. Plot of Stokes shift versus Lippert's polarity parameters.

constructed (Fig. 6) for the normal fluorescence using the following equation:

$$\bar{\upsilon}_{ss} = \bar{\upsilon}^{ab}_{max} - \bar{\upsilon}^{fl}_{max} = \text{const} + \left[\frac{2(\mu_e - \mu_g)^2}{hca^3}\right] f(D, n),$$

$$f(D, n) = \frac{D-1}{D-2} - \frac{n^2-1}{2n^2+1}$$

where $f(D, n)$ indicates the orientation polarizability and depicts the polarity parameter of the solvent, n the refractive index, D the dielectric constant, μ_e and μ_g the dipole moments of the fluorophore in the S_0 and S_1 states, respectively, h the Planck's constant, c the velocity of light, and a the Onsager's cavity radius. The values of $\bar{\upsilon}^{ab}_{max}$ were obtained from the fluorescence excitation spectra recorded in different solvents, using the λ_{em} of the SW fluorescence band. The Lippert plot is linear for the non-polar and polar/aprotic solvents with correlation coefficient of 1.1. This is on the expected lines because the Lippert plot does not take into account the specific interactions. The change in the dipole moment for the SW emission band obtained from the slope of the Lippert plot and taken a to be 0.436 nm, came out to be 1.83 D. Using the value of μ_g as 5.99 D (Table 1), the value of $\mu_e = 7.82$ D. This value is quite close to the data obtained from the CNDO/S-CI calculations for the rotamer a-1 in the S_1 state.

4.4. Excited state lifetimes

The excited state lifetimes for the SW fluorescence band were measured by exciting at 311 nm and monitoring at 355 nm in three solvents, whereas for the LW fluorescence band, it was carried out by using $\lambda_{exc} = 337$ nm and monitoring at the respective band maximum in four solvents. In each case, the fluorescence intensity followed a single exponential decay and the respective lifetime is compiled in Table 4. The values of radiative (k_r) and non-radiative (k_{nr}) rate constants for the LW fluorescence band were calculated using the following equations:

$$k_r = \frac{\phi_{fl}}{\tau_f}, \qquad k_{nr} = \frac{1}{\tau_f} - k_r$$

The values of ϕ_{fl} used in these relations for the LW fluorescence band were obtained by exciting the solutions at 330 nm. The similar rate constants for the SW fluorescence band were not determined because the ϕ_{fl} for this band could not be measured accurately. The data is compiled in Table 4.

4.5. Binary solvents

The effect of solvent polarity and hydrogen bonding on the fluorescence intensities of the SW and LW bands was studied by taking mixed solvents, e.g. dioxane/acetonitrile, dioxane/methanol and acetonitrile/methanol, and using 310 and 340 nm as the excitation wavelengths. Figs. 7 and 8 give the plot of the respective fluorescence intensities versus composition of the solvents (V/V). The decrease in the fluorescence intensity of the tautomer band of 2-HPIP-c is nearly independent of the λ_{exc} in dioxane/acetonitrile and dioxane/methanol mixtures. The decrease in the fluorescence intensity of the tautomer band is less in the former mixture ($59 \pm 3\%$) than that in the latter mixture ($77 \pm 2\%$). On the other hand, the fluorescence intensity of the SW band increases in both the mixtures up to 50 and 70%, respectively, and then decreases with increase in the acetonitrile or methanol and using $\lambda_{exc} = 310$ nm. The variation of the fluorescence intensity of the SW band of 2-HPIP-c as

Table 4
Lifetimes (τ, ns), fluorescence quantum yield (ϕ^T_{fl}), radiative rate constant (k_r, 10^7 s^{-1}) and non-radiative rate constant (k_{nr}, 10^7 s^{-1})

Solvents	τ^N	τ^T	(ϕ^T_{fl})	k_r	k_{nr}
Cyclohexane	–	2.43	0.199	9.1	37.2
Acetonitrile	1.0	1.27	0.934	7.4	71.1
Methanol	0.34	1.74	0.065	3.7	53.8
Water, pH = 6.6	–	0.93	–	–	

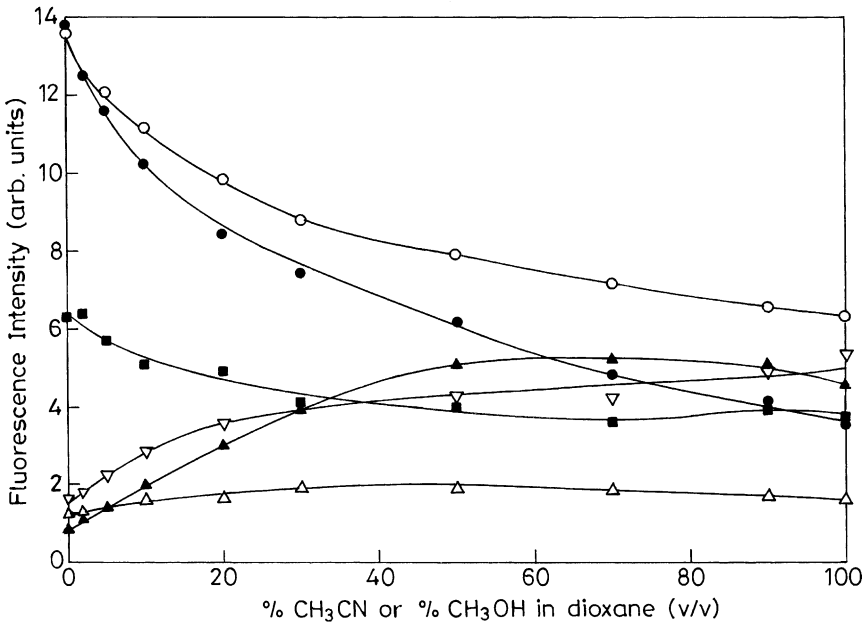

Fig. 7. Plot of fluorescence intensities of tautomer (○) and normal (△) bands in dioxane/acetonitrile; tautomer (●) and normal (▲) bands in dioxane/methanol; tautomer (■) and normal (▽) bands in acetonitrile/methanol solvent mixtures (λ_{exc} = 315 nm).

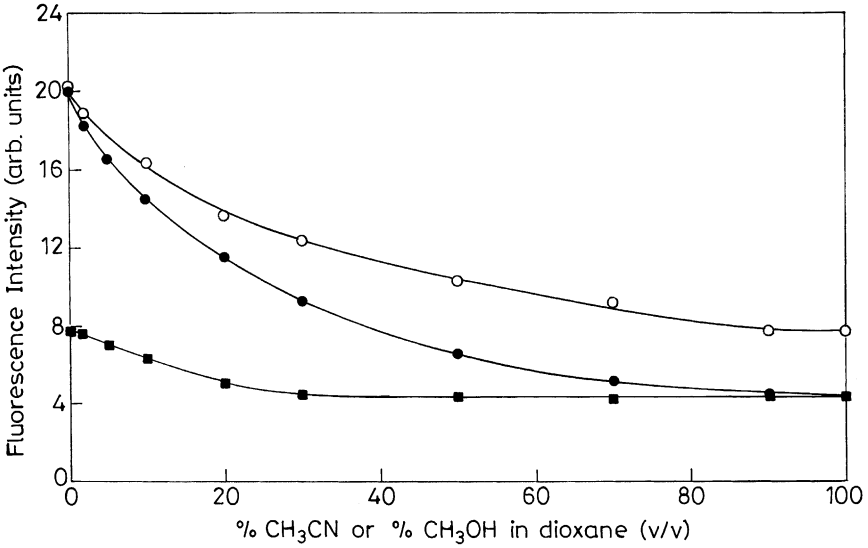

Fig. 8. Plot of fluorescence intensities of tautomer band (○) in dioxane/acetonitrile; (●) in dioxane/methanol; (■) in acetonitrile/methanol solvent mixtures (λ_{exc} = 340 nm).

a function of solvent composition is different from that of 2-HPIP-b [41], but similar to that observed for 2-HPBI [29].

5. Discussions

Based on earlier results and conclusions, it may be mentioned here that the rotamer a-1 or rotamer b-1 is responsible for the SW fluorescence band and rotamer a-2 or b-2 exhibits LW fluorescence band because ESIPT, leading to the formation of the tautomer, is only possible in the latter set of rotamers.

In all six species (two isomers, 'a' and 'b'; and three species of each isomer, a-1, a-2, T_a; b-1, b-2 and T_b, Scheme 2) were considered for the semi-empirical quantum mechanical calculations. The results of Table 1 have clearly shown that all the respective species of isomer 'a' are more stable than those of isomer 'b' (howsoever small it may be) and the stability of the respective species of isomer 'a' further increases with the increase of the polarity of the

solvents in S_0 state. This is because μ_g of each species of isomer 'a' is larger than that of the respective species of isomer 'b'. From the above results, it can be concluded that the species T_a and T_b will be absent in the S_0 state as these are highly unstable ($\sim$45 kJ mol^{-1}) with respect to their rotamers. On the other hand, in comparison to rotamer a-1, the other rotamers a-2, b-1 and b-2 are unstable by 3.6, 2.7 and 6.2 kJ mol^{-1}, respectively, under isolated conditions. Thus based on the heat of formation, total energies (under isolated and solvated conditions) and the spectral transitions data, it is very difficult to conclude the presence of either isomer 'a' or isomer 'b' or both. This is also substantiated by the fact that the activation energy for the interconversion of a-1 to a-2 or b-1 to b-2 is only 7.72 and 8.5 kJ mol^{-1}, respectively in the S_0 state.

Solvatochromic effect (Fig. 6) has shown that the μ_e for the species responsible for the SW fluorescence is 7.82 D. This value of μ_e is quite close to that of rotamer a-1, predicted by CNDO/S-CI for the S_1 state (7.76 D). On the other hand, the values of μ_g (5.30 D) and μ_e (5.42 D) for the rotamer b-1 are nearly similar to each other. Thus based on these values of dipole moments of rotamer b-1, the fluorescence band maximum for the normal emission of 2-HPIP-c would have been invariant to the nature of the solvents. Based on our results (Table 3), it may be concluded that rotamer a-1 is the only species present in non-polar and polar/aprotic solvents and is responsible for the SW fluorescence spectrum. This is further substantiated by the single exponential decay for the SW fluorescence and similar fluorescence excitation spectra obtained at different emission wavelengths of the SW fluorescence band. Similarly from the following observations, it may also be concluded that a-2 is the only species which is responsible for the LW (tautomer) fluorescence and not rotamer b-2, i.e. based on the results of Table 1, the dipole moments of T_a in the S_0 and S_1 states ($\mu_g = 4.78$ D and $\mu_e = 4.98$ D, obtained from the CNDO/S-CI calculations) are quite close to each other and thus the LW fluorescence band maximum will be nearly invariant to the solvent polarity. Whereas those of T_b are 3.1 and 3.99 D, respectively and thus small red shift should have been observed in the LW fluorescence band maximum under the similar conditions. Our results contradict this.

Having established that only one isomer 'a' of 2-HPIP-c is present in the solutions in the S_0 state, the spectral characteristics so obtained can be assigned as follows. The SW structured fluorescence originated from the rotamer a-1 and its fluorescence excitation band maxima in dioxane are at 302 and 313 nm and in methanol, these are at 304 and 318 nm. The LW broad structureless emission can be assigned to T_a, obtained from rotamer a-2 by ESIPT process and its fluorescence excitation band maxima in dioxane are at 322 and 329 nm and in methanol at 319 and 326 nm, respectively. The absorption spectrum so obtained is the composite absorption spectra of these two rotamers present in the S_0 state. The above assignments and other results can be supplemented from the following observations.

(i) Under isolated conditions and in the presence of polar solvents, rotamer a-1 is the most stable in comparison to rotamer a-2 and T_a by 3.6 and 44.8 kJ mol^{-1}, respectively. Tautomer T_a will not be present in the S_0 state, whereas both the rotamers a-1 and a-2 will be present in the S_0 state as the activation barrier for the interconversion of a-1 to a-2 is only 7.72 kJ mol^{-1} under isolated conditions.

(ii) As mentioned earlier, ESIPT process is not possible in rotamer a-1 (also substantiated by the charge densities at N_1 in the S_0 (5.2120) and S_1 (5.2273) states, which are nearly similar) the SW fluorescence band is assigned to it in all the solvents. This is further substantiated by: (a) similar excitation spectra at different λ_{em} in the SW fluorescence spectra, (b) single exponential decay, and (c) small Stokes shift observed in non-polar solvents. In polar/protic solvents, due to the competition between inter- and intramolecular hydrogen bonding, one may expect the presence of open solvated structure a-3. Our results suggest that the lifetime of the rotamer a-3 will be either similar to that of rotamer a-1 or there is an equilibrium present in the S_1 state between the rotamer a-1 and solvated structure a-3.

(iii) Large Stokes shifted LW fluorescence band suggests that this emission has originated from the species which is not present in the S_0 state and large geometrical changes have taken place in the species when excited to S_1 state. We assign this fluorescence to T_a, which is formed from the rotamer a-2 by ESIPT process. This process must be very fast (in ps range), because a single exponential decay has been observed in the LW fluorescence band of 2-HPIP-c in all the solvents in our ns time dependence spectrofluorimeter. This transformation of rotamer a-2 to T_a is substantiated by the fact as follows. (a) Charge density on N_3 increases from 5.1381 in the S_0 state to 5.3071 in the S_1 state. In other words, the basicity of N_3 atom increases on excitation to S_1 state. (b) The bond length of C_2–C_{10} in T_a (0.1403 nm) is shorter than that of in a-2 (0.1464 nm). (c) The results of Fig. 2, which represents the potential energy surface for IPT of 2-HPIP-c in S_0 and S_1 states as a function of distance between R(O_{16}–H_{17}), suggests that the formation of T_a from a-2 is an endothermic process in S_0 state and an exothermic process in the S_1 state. In other words, IPT process is thermodynamically unfavorable in the S_0 state, but becomes favorable in the S_1 state. The activation barrier for the IPT process is very large (107 kJ mol^{-1}) in the S_0 state in comparison to that in the S_1 state (67 kJ mol^{-1}). Although the activation barrier found for the IPT process is very large as compared to that obtained experimentally, an appreciably lowering of the activation barrier in the S_1 state suggests that IPT process is more favorable in S_1 state as compared to that in the S_0 state. Similar disagreements between the activation energies predicted

by theoretically and obtained experimentally have also been observed in nearly all the cases [8,68–71].

(iv) Dual emission is observed from two distinctly different species, having different precursors in the S_0 state and not by interconversion of one species into the other in the S_1 state. This is substantiated by: (a) different lifetimes for the SW and LW emission bands; (b) the large activation barrier (72.4 kJ mol^{-1}) for the interconversion of rotamer a-1 to a-2 in the S_1 state as compared to 7.72 kJ mol^{-1} in the S_0 state (Fig. 1). This also suggests that the equilibrium is not established between the two rotamers in the S_1 state during their lifetimes.

(v) There are three different parameters which can affect the fluorescence intensity of the fluorophore: (a) population of the rotamers a-1 and a-2, (b) polarity, and (c) hydrogen bonding capacity of the solvents. Based on the Maxwell–Boltzmann's distribution, the additional stability of rotamer a-1, will increase its population over rotamer a-2 in polar solvents by a factor of exp(-$\Delta E/RT$), i.e. population of rotamer a-1 increases by 20% and that of rotamer a-2 decreases by 77% in methanol as a solvent when compared to that in dioxane or cyclohexane. The fluorescence intensity of the tautomer band decreases with increase in the percentage composition of acetonitrile in dioxane/acetonitrile mixture. Acetonitrile being an aprotic solvent, decrease in the tautomer emission is thus due to the increase in the polarity of the medium. Similar behavior has also been observed in other systems [72,73]. Since the polarity parameters of acetonitrile and methanol are not very different form each other, the additional decrease in the tautomer emission in dioxane/methanol or acetonitrile/methanol mixtures is due to the specific interaction between the fluorophore and solvent molecules. In protic solvents, like alcohols, there can be a competition between the inter- and intramolecular hydrogen bonding in rotamer a-2 in particular and in rotamer a-1 in general. This leads to an open solvated structure a-3, where ESIPT is not possible and may give rise to normal emission. Above results support that increase in the polarity of the medium plays the major role in the decrease in the tautomer emission rather hydrogen bonding. This is also reflected by the fact the fluorescence quantum yield of the tautomer band increases in going from methanol to propanol, which is even greater than that in acetonitrile. This is supported by the fact that the value of k_{nr} in acetonitrile is greater than that in methanol (Table 4). On other hand, the large increase in the normal emission in protic solvents (a factor of 6 in dioxane/methanol mixture) cannot be accounted for simply due to the increase in the population of the rotamer a-1 by the polarity factor (only 20%). As said above, an additional increase in the normal emission arises from the open structure a-3, formed from a-2 by disrupting the intramolecular bond between =N and hydroxyl proton. Similar increase in the normal emission has also been observed in other systems and a similar mechanism can be proposed [74]. The large decrease in the tautomer emission observed in 2-HPIP-b in protic solvents in comparison to 2-HPIP-c is due to the weaker intramolecular hydrogen bonding in the former as reflected by the following data. The dihedral angle φ and the bond length between the imidazole nitrogen atom and the hydroxyl proton in 2-HPIP-b are 43° and 0.234 nm and similar values in 2-HPIP-c are 30° and 0.230 nm.

(vi) Lastly large blue shifted fluorescence band (458 nm) observed in water as compared to that in other organic solvents (477 nm) could not be assigned to the tautomer band, because there is hardly any difference in the values of μ_g and μ_e which can lead to large blue shift in fluorescence spectrum. This is shown by the LW emission in other solvents. Further the fluorescence excitation spectra recorded at 450 nm emission wavelength resemble with the absorption spectrum. As said earlier, this band can be assigned to the zwitterions but the detailed study is in progress and will reported later.

6. Conclusions

From the above results, the following conclusions can be made. (i) Based on the semi-empirical quantum mechanical calculations and solvatochromic effects, the isomer 'a' is the only species with rotamer a-1 and rotamer a-2 present in the S_0 state. (ii) Dual emission is observed by exciting the individual species in the S_0 state and the interconversion between the two rotamers is not possible in the S_1 state. This is supported by different excited state lifetimes for each species and very large activation barrier for the interconversion of rotamer a-1 to rotamer a-2 in the S_1 state as compared to that in the S_0 state. (iii) The normal emission in non-polar and polar/protic solvents can be assigned to the rotamer a-1, whereas in polar/protic solvents, the contribution to the normal emission is also made by the rotamer a-3. (iv) The tautomer emission can be assigned to the tautomer T_a, formed by the ESIPT in the rotamer a-2. (v) AM1 calculations have shown that thermodynamically and kinetically, the IPT in the enol → keto tautomerization is more favorable in the S_1 state than that in the S_0 state. (vi) Polarity of the solvents plays major role in decreasing in the tautomer emission than the specific interactions. (vii) Fluorescence spectrum in water at pH 6.6 can be assigned to the zwitterions. This behavior is different from that observed in other similar systems. Detailed analysis will be presented later.

Acknowledgements

We are thankful to the Department of Science and Technology, New Delhi, for the financial support to the project number SP/S_1/H-07/2000.

References

[1] S.J. Formosinho, L.G. Arnaut, J. Photochem. Photobiol. A 75 (1993) 1 and references listed there in.
[2] L.G. Arnaut, S.J. Formosinho, J. Photochem. Photobiol. A 75 (1993) 21.
[3] S.M. Ormson, R.G. Brown, Prog. React. Kinet. 19 (1994) 45.
[4] D. Legourrieve, S.M. Ormson, R.G. Brown, Prog. React. Kinet. 19 (1994) 211.
[5] M. Kasha, J. Chem. Soc., Faraday Trans. 2 82 (1986) 2379.
[6] M. Wiechmann, H. Port, W. Frey, F. Larmer, T.J. Elsaesser, J. Phys. Chem. 95 (1991) 1918.
[7] H. Eisenberger, B. Nickel, A.A. Ruth, W. Al-Soufi, K.H. Grellmann, M. Novo, J. Phys. Chem. 95 (1991) 10509.
[8] F. Rodriguez-Prieto, M.C.R. Rodriguez, M.M. Gonzale, M.A.R. Fernandez, J. Phys. Chem. 98 (1994) 8666.
[9] A. Douhal, F. Amat-Guerri, U. Acuna, J. Phys. Chem. 99 (1995) 76.
[10] A. Douhal, F. Lahanami, A.H. Zewail, Chem. Phys. 207 (1996) 477.
[11] M. Brauer, M. Mosquera, J.L. Perez-Lustres, F. Rodriguez-Prieto, J. Phys. Chem. 102 (1998) 10736.
[12] C. Chudoba, E. Riede, M. Pfeiffer, T. Elsaesser, Chem. Phys. Lett. 263 (1996) 622.
[13] M.C.R. Rodriguez, F. Rodriguez-Prieto, M. Mosquera, Phys. Chem. Chem. Phys. 1 (1999) 253 and references listed there in.
[14] M. Mosquera, J.C. Penedo, M.C.R. Rodriguez, F. Rodriguez-Preito, J. Phys. Chem. 100 (1996) 5398.
[15] A.U. Acuna, F. Amat, J. Catalan, A. Costela, J.M. Figuera, J.M. Munoj, Chem. Phys. Lett. 132 (1986) 567.
[16] A. Costela, F. Amat, J. Catalan, A. Douhal, J.M. Figuera, J.M. Munoj, A.U. Acuna, Opt. Commun. 64 (1987) 457.
[17] A. Costela, J.M. Munoj, A. Douhal, J.M. Figuera, A.U. Acuna, Appl. Phys. B 49 (1989) 545.
[18] D.B. O'Connor, G.W. Scott, D.R. Coulter, A. Yavrouln, J. Phys. Chem. 95 (1991) 10252.
[19] P.T. Chou, M.L. Martinej, Radiat. Phys. Chem. 41 (1993) 373.
[20] L.A. Hauch, C.L. Renschlar, Nucl. Instr. Meth. A 235 (1985) 41.
[21] T. Nishiya, S. Yamuchi, N. Hirota, M. Baba, I. Hamazaki, J. Phys. Chem. 90 (1986) 5730.
[22] A. Syntnik, J. Carlos Devella, J. Phys. Chem. 99 (1995) 13208.
[23] S. Santra, S.K. Dogra, J. Photochem. Photobiol. A 101 (1996) 221.
[24] E.L. Roberts, J.K. Dey, I.M. Werner, J. Phys. Chem. A 100 (1996) 19681.
[25] E.L. Roberts, J.K. Dey, I.M. Werner, J. Phys. Chem. A 101 (1997) 5296.
[26] S.K. Das, A. Bansal, S.K. Dogra, Bull. Chem. Soc. Jpn. 70 (1997) 307.
[27] S.K. Das, S.K. Dogra, J. Chem. Soc., Faraday Trans. 94 (1998) 139.
[28] S.K. Das, S.K. Dogra, J. Colloid Int. Sci. 205 (1998) 443.
[29] H.K. Sinha, S.K. Dogra, Chem. Phys. (1986) 317.
[30] M. Krishnamoorthy, S.K. Dogra, J. Photochem. 32 (1986) 235.
[31] A.K. Mishra, S.K. Dogra, J. Photochem. 31 (1985) 333.
[32] J.K. Dey, S.K. Dogra, Chem. Phys. 149 (1990) 97.
[33] J.K. Dey, S.K. Dogra, Bull. Chem. Soc. Jpn. 64 (1991) 3142.
[34] J.K. Dey, S.K. Dogra, J. Photochem. Photobiol. A 66 (1992) 15.
[35] J.K. Dey, S.K. Dogra, Can. J. Chem. 69 (1991) 635.
[36] S. Santra, S.K. Dogra, Chem. Phys. 226 (1998) 285.
[37] S.K. Das, G. Krishnamoorthy, S.K. Dogra, Can. J. Chem. 78 (2000) 191.
[38] S. Santra, G. Krishnamoorthy, S.K. Dogra, J. Phys. Chem. A 104 (2000) 476.
[39] S. Santra, G. Krishnamoorthy, S.K. Dogra, Chem. Phys. Lett. 311 (1999) 55.
[40] S. Santra, G. Krishnamoorthy, S.K. Dogra, Chem. Phys. Lett. 327 (2000) 230.
[41] G. Krishnamoorthy, S.K. Dogra, J. Lumin. 92 (2001) 91.
[42] E. Fasani, A. Albini, P. Savarino, G. Viscardi, E. Barni, J. Heterocyclic Chem. 30 (1993) 1041.
[43] G. Krishnamoorthy, S.K. Dogra, Spectrochim. Acta A 301 (1999) 2647.
[44] M. Krishnamoorthy, P. Phaniraj, S.K. Dogra, J. Chem. Soc., Perkin Trans. II (1986) 1917.
[45] H.K. Sinha, S.K. Dogra, J. Chem. Soc., Perkin Trans. II (1987) 1564.
[46] A.K. Mishra, S.K. Dogra, Spectrochim. Acta A 39 (1983) 973.
[47] A.K. Mishra, M. Swaminathan, S.K. Dogra, J. Photochem. 26 (1984) 49.
[48] R.W. Middleton, D.G. Wibberly, J. Heterocyclic Chem. 17 (1980) 1757.
[49] J.A. Riddick, W.B. Bunger, Organic Solvents, Wiley, New York, 1970.
[50] G. Krishnamoorthy, S.K. Dogra, J. Org. Chem. 64 (1999) 6566.
[51] G.G. Guilbault, Practical Fluorescence, Marcel Dekker, New York, 1971, p. 13.
[52] H. Hinze, H.H. Jaffe, J. Am. Chem. Soc. 84 (1962) 540.
[53] M.J.S. Dewar, E.G. Zeoblish, E.F. Healy, J.J. Stewart, J. Am. Chem. Soc. 107 (1985) 3902.
[54] Th. Arthen-Engeland, T. Bultmann, N.P. Earnsting, M.A. Roderiguez, W. Theil, Chem. Phys. 163 (1992) 43.
[55] J. Catalan, F. Fabero, M.S. Guijarro, R.M. Claramunt, M.D. Santa Marria, M. de la Concepcion Foces-Foces, F.H. Cano, J. Elguero, R. Sastra, J. Am. Chem. Soc. 112 (1990) 746.
[56] B. Dick, J. Phys. Chem. 94 (1990) 5752.
[57] P. Purkayastha, P.K. Bhattacharyya, S.C. Bera, N. Chattopadhyay, Phys. Chem. Chem. Phys. 1 (1999) 3235.
[58] J. Delbene, H.H. Jaffe, J. Chem. Phys. 48 (1989) 1807.
[59] A. Kumar, P.C. Mishra, QCPE Bull. 9 (1989) 67.
[60] N. Mataga, T. Kubata, Molecular Interactions and Electronic Spectra, Marcel Dekker, New York, 1970.
[61] J.F. Letard, R. Lepouyade, W. Rettig, Chem. Phys. Lett. 222 (1994) 209.
[62] E. Lippert, Z. Electrochem. 61 (1957) 962.
[63] M.M. Balamurali, S.K. Dogra, Unpublished result.
[64] M.C.R. Roderiguez, J.C. Penedo, R.J. Willemse, M. Mosquera, F. Roderiguez-Prieto, J. Phys. Chem. A 103 (1999) 7236.
[65] L.S. Rosenberg, J. Simons, S.G. Schulman, Talanta 26 (1979).
[66] E. Lippert, Z. Electrochem. 61 (1957) 962.
[67] N. Mataga, Y. Kaifu, Y. Koizumi, Bull. Chem. Soc. Jpn. 29 (1956) 465.
[68] F. Marquez, I. Zabala, F. Tomas, Anales de Qumica 91 (1995) 647.
[69] P. Purkayastha, N. Chattopadhyay, Phys. Chem. Chem. Phys. 2 (2000) 203.
[70] S. Maheshwari, A. Chowdhury, N. Sathyamurthy, H. Mishra, H.B. Tripathi, M. Pande, J. Chandrasekhar, J. Phys. Chem. 103 (1999) 6257.
[71] H. Mishra, H.C. Joshi, H.B. Tripathi, S. Maheshwari, N. Sathyamurthy, M. Pande, J. Chandrasekhar, J. Photochem. Photobiol. A 139 (2001) 23.
[72] P.T. Chou, M.L. Martinez, W.C. Cooper, D. McMorrow, S.T. Coline, M. Kasha, J. Phys. Chem. 96 (1992) 5203.
[73] Y. Chen, P.L. Petrich, J. Phys. Chem. 97 (1993) 1770.
[74] F. Gai, R.L. Rich, J.W. Petrich, J. Am. Chem. Soc. 16 (1994) 735.